Robustness Analysis of DNA-based Biomolecular Feedback Controllers to Parametric and Time Delay Uncertainties

Rucha Sawlekar, Mathias Foo, and Declan G. Bates

***Abstract*— Recent advances in DNA computing have greatly facilitated the design of biomolecular circuitry based on DNA strand displacement reactions. An important issue to consider in the design process for such circuits is the effect of biological and experimental uncertainties on the functionality and reliability of the overall circuit. In the case of biomolecular feedback control circuits, such uncertainties could lead to a range of adverse effects, including achieving wrong concentration levels, sluggish performance and even instability. In this paper, we analyse the robustness properties of two biomolecular feedback controllers; a classical linear proportional integral (PI) and a recently proposed nonlinear quasi sliding mode (QSM) controller, subject to uncertainties in the experimentally implemented rates of their underlying chemical reactions, and to variations in accumulative time delays in the process to be controlled. Our results show that the nonlinear QSM controller is significantly more robust against investigated uncertainties, highlighting its potential as a practically implementable biomolecular feedback controller for future synthetic biology applications.**

I. INTRODUCTION

A design framework that uses abstract *chemical reaction networks* (CRNs) as a programming language to implement enzyme-free, enthalpy–entropy driven DNA elementary reactions [1] has recently attracted much attention in the synthetic biology community [2]-[4]. The designed circuitry is implementable in DNA by means of a toehold-mediated DNA strand displacement (DSD) mechanism, through the well-known Watson-Crick base-pairing (i.e. adenine-thymine and guanine-cytosine) [5]. The selection of appropriate DNA sequences allows precise control over the dynamics of the implemented DNA reactions, thus facilitating an accurate molecular programming of the desired function, operator or circuit. Also, design of synthetic circuits using this approach is now being facilitated by sophisticated CAD tools, such as the Visual DSD software package [6]. Examples of successfully designed and implemented biomolecular circuitry using this approach include linear and nonlinear feedback controllers [4], [7], [8], dynamics of predator-prey systems [9], and oscillators [10].

In recent work we have developed a nonlinear QSM controller [7] using four activation-deactivation CRNs inspired by the ultrasensitive behaviour exhibited by *mitogen activated protein kinase* (MAPK) cascade [11] and implemented using the DSD mechanism. An important requirement for any embedded bimolecular controller is that its design provides robustness to various forms of uncertainty and variability that could arise in its final implementation in DNA. Here, we focus on two important sources of such uncertainty - variability in the rate constants of the abstract chemical reactions underlying the closed-loop control system, and uncertain time delays in the biomolecular process to be controlled. In practice, experimental biologists are rarely able to specify the reaction rates of chemical reactions exactly, and additionally, as highlighted in [8], unregulated chemical devices or leaky expression can potentially affect production and degradation rates and subsequently alter the behaviour of the designed components. There are also many reasons why we might wish to include time delays in CRN models of biomolecular processes, since this avoids cataloging potentially large numbers of intermediate species and their reactions, in favour of describing the dynamic relationships between the concentrations of key species. As a result, fewer concentration variables will generally be required, thus simplifying the overall circuit design problem. Also, in preliminary investigations of a new system, the level of description afforded by a low-order time delayed CRN model is often closer to our state of knowledge than is a detailed model, in which a certain amount of speculation about intermediate species is required, [15].

R. Sawlekar, M. Foo, and D. G. Bates are with the Warwick Centre for Integrative Synthetic Biology, School of Engineering, University of Warwick, Coventry, CV4 7AL, United Kingdom, R.Sawlekar@warwick.ac.uk, M.Foo@warwick.ac.uk, D.Bates@warwick.ac.uk

II. SYSTEM DESCRIPTION AND METHODOLOGY

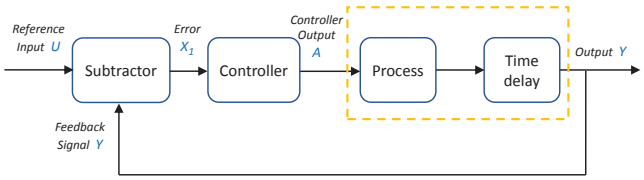

Fig. 1: The biomolecular closed-loop feedback control system with the accumulative process time delay.

The system configuration considered here is shown in Fig. 1, that is a biomolecular closed-loop feedback circuit consisting of a number of dynamic components, namely, a subtractor, a controller and a second order nonlinear biomolecular process with an accumulative time delay. The controller analysed here is a nonlinear *quasi sliding mode* (QSM) controller, adapted from [12] - for the purposes of comparison, we also illustrate the level of performance that is achieved using a classical linear *proportional integral* (PI) controller.

Whereas signals in systems theory can take both positive and negative values, biomolecular concentrations can only

978-1-5090-2959-4/16/$31.00 ©2016 IEE

take non-negative values. To resolve this difficulty, following the approach in [8] and [14], we represent a signal x as the difference in concentrations of two DNA strands, such that $x = x^+ - x^-$. Here, x^+ and x^- are respectively the positive and negative components of x. In this paper, $x_i^{\pm} \xrightarrow{k} x_o^{\pm}$ denotes the set of the following two reactions: $x_i^+ \xrightarrow{k} x_o^+$ and $x_i^- \xrightarrow{k} x_o^-$.

The abstract chemical reactions describing the QSM controller in Fig. 1, are given by:

$$X_1^{\pm} + B^{\pm} \xrightarrow{k_{b_1}} X_2^{\pm}, \quad (1a) \qquad A^{\pm} + X_3^{\pm} \xrightarrow{k_{b_2}} X_4^{\pm}, \quad (1e)$$
$$X_2^{\pm} \xrightarrow{k_{c_1}} A^{\pm} + X_1^{\pm}, \quad (1b) \qquad X_4^{\pm} \xrightarrow{k_{c_2}} B^{\pm} + X_3^{\pm}, \quad (1f)$$
$$X_2^{+} + X_2^{-} \xrightarrow{\eta} \phi, \quad (1c) \qquad X_4^{+} + X_4^{-} \xrightarrow{\eta} \phi, \quad (1g)$$
$$A^{+} + A^{-} \xrightarrow{\eta} \phi, \quad (1d) \qquad B^{+} + B^{-} \xrightarrow{\eta} \phi. \quad (1h)$$

where, X_1 is the input and A is the output of the QSM controller. The above CRNs realise an ultrasensitive switch-like input-output response that approximates an ideal sliding mode controller [16]-[18]. By tuning the concentration of the DNA strands $X_3^{\pm}$, the input-output response of the set of CRNs can be made to closely approximate the ideal switch implemented by a *sliding mode controller* (SMC) [16]-[18], so that it implements a QSM controller. Here, k_{b_1} and k_{b_2} denote the binding reaction rates whereas k_{c_1} and k_{c_2} denote the catalytic reaction rates and η is the annihilation rate. The tuning of the QSM controller involves adjusting k_{b_1}, k_{b_2}, k_{c_1} and k_{c_2}. Now, using mass action kinetics (see eg. [19]), the set of reactions given by Eqns. (1) may be represented by the following set of ODEs:

$$\frac{dA}{dt} = k_{c_1}X_2 - k_{b_2}AX_3, \quad (2a) \qquad \frac{dB}{dt} = -k_{b_1}X_1B + k_{c_2}X_4, \quad (2c)$$
$$\frac{dX_2}{dt} = k_{b_1}X_1B - k_{c_1}X_2, \quad (2b) \qquad \frac{dX_4}{dt} = k_{b_2}AX_3 - k_{c_2}X_4. \quad (2d)$$

From Eqns. (2), we can see that $S_{qsm} \doteq A + B + X_2 + X_4$ is constant. Thus, the signal B is variable and depends on the dynamic signals A, X_2 and X_4. Since, X_1 also varies over time; this means that the term $k_{b_1}X_1B$ in Eqn. (2b) is nonlinear. The linear PI controller is constructed following the approach of [8] and [4] using three CRNs for the integration and seven for the proportional gain as:

[Integrator]: $X_1^{\pm} \xrightarrow{k_I} X_1^{\pm} + X_2^{\pm}$, (3a) $\qquad X_2^{+} + X_2^{-} \xrightarrow{\eta} \phi$. (3b)

[Proportional]:
$$X_1^{\pm} \xrightarrow{k_p} X_1^{\pm} + A^{\pm}, \quad (4a) \qquad A^{\pm} \xrightarrow{k_d} \phi, \quad (4c)$$
$$X_2^{\pm} \xrightarrow{k_c} X_2^{\pm} + A^{\pm}, \quad (4b) \qquad A^{+} + A^{-} \xrightarrow{\eta} \phi. \quad (4d)$$

Here, the signal X_1 is the input and A is the output. Furthermore, k_p and k_c denote the catalytic reaction rates while k_d denotes the degradation rate. Using mass action kinetics, the following ODE representation is obtained for the PI controller:

$$\frac{dX_2}{dt} = k_I X_1, \quad (5a) \qquad \frac{dA}{dt} = k_p X_1 + k_c X_2 - k_d A. \quad (5b)$$

We consider a second order nonlinear process that can be formed using a combination of unimolecular and bimolecular CRNs, given as follows:

$$A^{\pm} + X_5^{\pm} \xrightarrow{k_{r_1}} X_6^{\pm}, \quad (6a) \qquad Y(t+\tau)^{\pm} \xrightarrow{k_{r_3}} \phi, \quad (6c)$$
$$X_6^{\pm} \xrightarrow{k_{r_2}} Y^{\pm} + X_5^{\pm}, \quad (6b) \qquad Y^{+} + Y^{-} \xrightarrow{\eta} \phi. \quad (6d)$$

where, k_{r_1}, k_{r_2}, k_{r_3} are binding, catalytic and degradation reaction rates, respectively. The input signal to the process module is A and the output is Y. The term τ in Eqn. (6c) indicates the accumulative time delay involved in the production of the output species Y. Applying mass action kinetics, we get:

$$\frac{dX_6}{dt} = k_{r_1}AX_5 - k_{r_2}X_6, \quad (7a) \qquad \frac{dY}{dt} = k_{r_2}X_6 - k_{r_3}Y(t-\tau). \quad (7b)$$

where, $X_{Total} \doteq X_5 + X_6$ is constant and conserved through the entire time of the process. For the closed-loop feedback control, we need a module to compute the difference of the reference signal (U) and output signal (Y). Following [8], [14] and as implemented in [12], the CRNs that perform the subtraction are given by:

$$U^{\pm} \xrightarrow{k_s} U^{\pm} + X_1^{\pm}, \quad (8a) \qquad X_1^{\pm} \xrightarrow{k_s} \phi, \quad (8c)$$
$$Y^{\pm} \xrightarrow{k_s} Y^{\pm} + X_1^{\mp}, \quad (8b) \qquad X_1^{+} + X_1^{-} \xrightarrow{\eta} \phi. \quad (8d)$$

where, k_s is the subtraction rate. Here, signals U and Y are the inputs and X_1 is the output of the subtractor. In other words, the value of signal X_1 being produced is equivalent to the difference between the two input signals, U and Y. In addition, both the catalysis reaction rates in Eqns. (8a) and (8b) are set to be equal to the degradation rate. Applying mass action kinetics to Eqns. (8) gives:

$$\frac{dX_1}{dt} = k_s(U - Y - X_1). \quad (9)$$

In the context of our feedback system shown in Fig. 1, the inputs to the subtractor comprise the reference input signal U and the process output Y while its output X_1 is used as the input to the controller.

III. SIMULATION RESULTS

The performance of the QSM controller with $\tau = 0$s and $\tau = 1000$s is shown in Fig. 2. In both the cases, the QSM controller is seen to accurately track the reference signal, with nearly the same settling time of approximately 12,000s. However, when the response of the PI controller is evaluated in the presence of $\tau = 1000$s, as shown in Fig. 2, large overshoots can be observed.

To analyse the robustness of closed-loop responses achieved with the QSM controller, a formal Monte Carlo simulation campaign was performed. All the parameters determining the rate constants of the chemical reactions underlying the closed-loop system are randomly drawn from a uniform distribution over repeated simulations. The number of Monte Carlo simulations required to achieve various

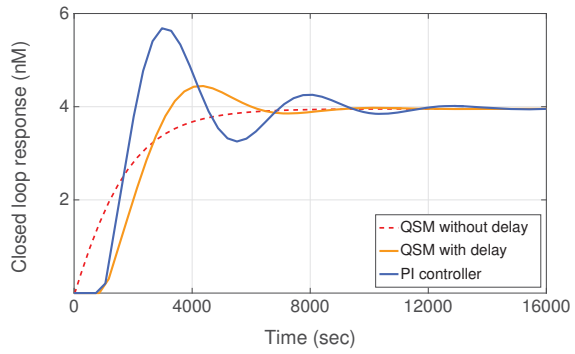

Fig. 2: Comparing system performance of QSM controller with PI controller for $\tau = 1000$s. The dashed line shows the response of the QSM controller for $\tau = 0$s.

levels of estimation uncertainty with known probability were calculated using the well-known Chernoff bound [20]. An accuracy of 0.05 and a confidence level of 90% were chosen for the Monte Carlo simulation analysis, which requires 1060 number of simulations, as discussed in [20]-[22]. To investigate the effect of different levels of uncertainty we varied the parameters within ranges of 20% and 50% around their nominal values. Mathematically, we have $p(1+\Delta P(x))$ where, $p \in \{k_s, k_{b_1}, k_{b_2}, k_{c_1}, k_{c_2}, k_I, k_p, k_c, k_d, k_{r_1}, k_{r_2}, k_{r_3}\}$, $P(x)$ is the probability distribution and $\Delta \in \{0.2, 0.5\}$.

In the simulations, the given step input U changes from 0 to 4 nM at time $t = 0$s and the role of the controller is to ensure that the process output Y tracks the reference input. As quantitative measures of control system performance, we measure the step response characteristics, which include settling time (t_s), rise time (t_r), percentage overshoot (M_{OS}) and steady state error (e_{ss}). It is desirable to achieve small values of t_s, t_r and M_{OS}, while $e_{ss} = 0$. We first calculate the closed-loop response without parameter uncertainty, i.e. with nominal parameter values to use it as a benchmark for comparison. Tables I and II detail the results of the Monte Carlo simulation campaign for both the QSM and PI controllers. The PI controller was observed to lose closed-loop stability for $\Delta = 0.5$. The worst case values of each of the step response characteristics and their associated parameter values are shown for each of the analysed uncertainty sets in Tables I and II. Ranges are shown for the uncertain parameters since their worst-case values for each step response characteristic are different, e.g. the parameters yielding the worst t_s may not yield the worst t_r, M_{os} and e_{ss} and vice versa. Figs. 3(a) and 3(b) show the step responses produced by the Monte Carlo simulation campaign for each controller when $\Delta = 0.2$ and similarly, Figs. 3(c) and 3(d) show the step responses when $\Delta = 0.5$. As shown, the QSM controller displays significantly greater robustness to the applied levels of uncertainty, highlighting its potential for successful experimental implementation.

TABLE I: Step response characteristics and worst-case parameter ranges for the PI controller.

Characteristics	Nominal	$\Delta = 0.2$	$\Delta = 0.5$
t_s (s)	12,652	15,958	unstable
t_r (s)	718	11,259	unstable
M_{OS} (%)	43.75	283.17	unstable
e_{ss} (M)	0	0	unstable
Parameters	**Nominal**	**$\Delta = 0.2$**	**$\Delta = 0.5$**
Subtractor			
k_s (/s) [10^{-3}]	2.4	2.714-2.831	2.863-3.530
PI controller			
k_I (/M/s) [10^{-6}]	1.6	1.616-1.907	1.631-2.110
k_p (/M/s)	0.2	0.232-0.233	0.272-0.299
k_c (/s) [10^{-4}]	1.6	1.722-1.894	1.934-2.351
k_d (/s) [10^{-1}]	3.2	3.255-3.364	3.223-4.497
Nonlinear process			
k_{r_1} (/M/s) [10^2]	5	5.732-5.926	6.951-7.455
k_{r_2} (/s)	1.6	1.818-1.884	1.804-2.242
k_{r_3} (/s) [10^{-6}]	8	8.033-8.696	9.561-11.335
Time delay			
τ (s)	1000	700-1118	695-1436

IV. CONCLUSIONS

Within the framework of CRNs, we designed an embedded synthetic biomolecular feedback circuit that can be implemented using enzyme-free, enthalpy and entropy driven DNA elementary reactions. We analyzed and compared the performance of a nonlinear QSM controller with a linear PI controller, when subjected to potential accumulative process time delays in the production of the output species of interest. We introduced different levels of uncertainty in the parameters representing the reaction rates of the underlying chemical reactions, and in the process time delay to investigate the robustness of both controllers to these variabilities. Our results highlight the strong robustness properties of the QSM controller, indicating its suitability for implementation in wet-lab experiments.

ACKNOWLEDGMENT

We gratefully acknowledge financial support from EPSRC via research grant EP/M002187/1, BBSRC via research grant

TABLE II: Step response characteristics and worst-case parameter ranges for the QSM controller.

Characteristics	Nominal	$\Delta = 0.2$	$\Delta = 0.5$
t_s (s)	9,654	15,562	15,954
t_r (s)	1,281	1,471	1,631
M_{OS} (%)	12.36	38.23	181.29
e_{ss} (M)	0	0	oscillatory
Parameters	**Nominal**	**$\Delta = 0.2$**	**$\Delta = 0.5$**
Subtractor			
k_s (/s) [10^3]	1	1.139-1.175	1.059-1.267
QSM controller			
k_{b_1} (/M/s) [10^{-3}]	40	41.060-47.587	40.642-59.807
k_{b_2} (/M/s) [10^{-3}]	40	43.094-47.103	42.489-54.347
k_{c_1} (/s) [10^3]	9	9.122-10.732	12.423-13.410
k_{c_2} (/s) [10^3]	10	10.201-11.946	10.269-14.694
Nonlinear process			
k_{r_1} (/M/s) [10^2]	5	5.077-5.900	5.038-7.185
k_{r_2} (/s)	1.6	1.769-1.884	1.651-2.368
k_{r_3} (/s) [10^{-6}]	8	9.040-9.310	9.079-11.390
Time delay			
τ (s)	1000	853-1169	853-1469

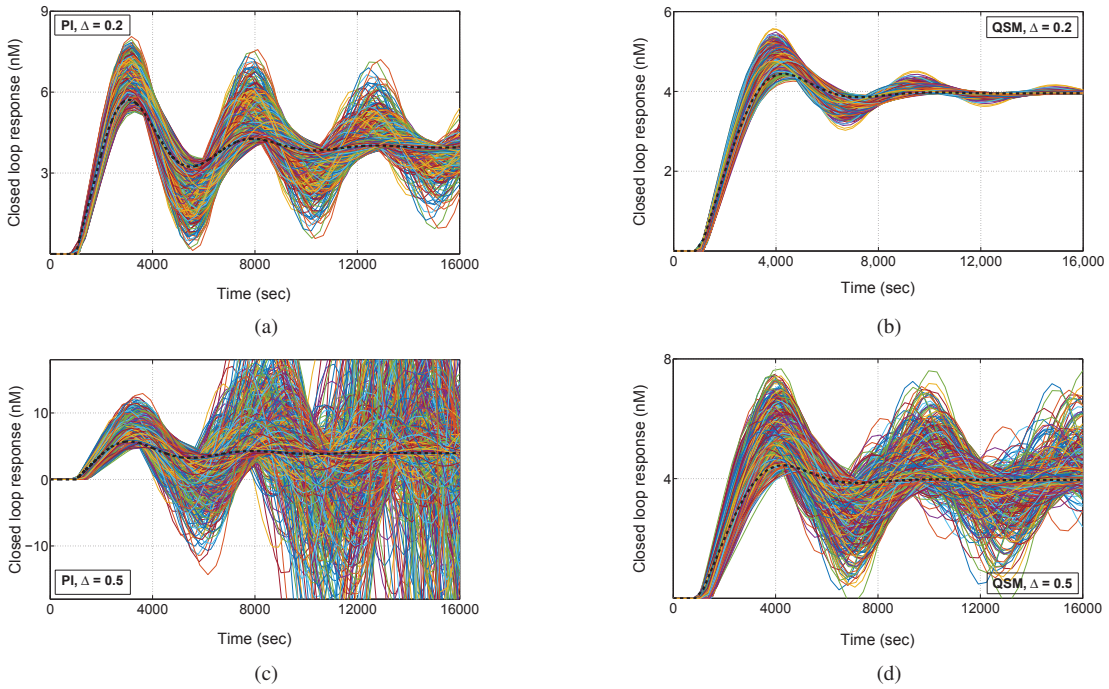

Fig. 3: Comparing system performance for 20% and 50% uncertainty in parameters and time delay; for the Monte Carlo simulation analysis (no. of simulations = 1060). Plots (a) and (b) are the closed-loop responses with the PI controller and the QSM controller, respectively, with $\Delta = 0.2$, Plots (c) and (d) are the closed-loop responses with the PI controller and the QSM controller, respectively, with $\Delta = 0.5$.

BB/M017982/1 and from the School of Engineering of the University of Warwick.

REFERENCES

[1] D. Soloveichik, G. Seelig and E. Winfree, "DNA as a Universal Substrate for Chemical Kinetics", *Proceedings of the National Academy of Sciences, USA*, vol. 107, no. 12, pp. 5393–5398, 2010.

[2] G. Seelig, D. Soloveichik, D.Y. Zhang and E. Winfree, "Enzyme-free Nucleic Acid Logic Circuits", *Science*, vol. 314, no. 5805, pp. 1585–1588, 2006.

[3] L. Qian and E. Winfree, "A Simple DNA Gate Motif for Synthesizing Large-Scale Circuits", *Journal of the Royal Society of Interface*, p.rsif20100729, 2011.

[4] B. Yordanov, J. Kim, R. Petersen, A. Shudy, V. Kulkarni and A. Phillips, "Computational Design of Nucleic Acid Feedback Control Circuits", *ACS Synthetic Biology*, vol. 3, no. 8, pp. 600–616, American Chemical Society, 2014.

[5] D. Zhang and E. Winfree, "Control of DNA Strand Displacement Kinetics using Toehold Exchange", *Journal of the American Chemical Society*, vol. 131, no. 47, pp. 17303–17314, 2009.

[6] M. R. Lakin, S. Youssef, F. Polo, S. Emmott and A. Phillips, "Visual DSD: A Design and Analysis Tool for DNA Strand Displacement Systems", *Bioinformatics*, vol. 27, no. 22, pp. 3211–3213, 2011.

[7] R. Sawlekar, F. Montefusco, V. Kulkarni, and D. G. Bates, "Biomolecular Implementation of a Quasi Sliding Mode Feedback Controller based on DNA Strand Displacement Reactions", *Proceedings of IEEE Engineering in Medicine and Biology Conference*, pp. 949–952. Milan, Italy, 2015.

[8] K. Oishi and E. Klavins, "Biomolecular Implementation of Linear I/O Systems", *IET Systems Biology*, vol. 5, no. 4, pp. 252–260, 2011.

[9] T. Fujii and Y. Rondelez, "Predator-Prey Molecular Ecosystems", *ACS Nano*, vol. 7, no. 1, pp. 27–34, 2013.

[10] M. Weitz, J. Kim, K. Kapsner, E. Winfree, E. Franco and F.C. Simmel, "Diversity in the Dynamical Behaviour of a Compartmentalized Programmable Biochemical Oscillator", *Nature Chemistry*, vol. 6, pp. 295-302, 2014.

[11] C. Gomez-Uribe, G. C. Verghese and L. A. Mirny, "Operating Regimes of Signaling Cycles: Statics, Dynamics, and Noise Filtering", *PLoS Computational Biology*, vol. 3, no. 12, pp. 2487-2497, 2007.

[12] R. Sawlekar, F. Montefusco, V. Kulkarni, and D. G. Bates, "Implementing Nonlinear Feedback Controllers using DNA Strand Displacement Reactions", *IEEE Transactions on Nanobioscience*, DOI: 10.1109/TNB.2016.2560764, 2016.

[13] D. Del Vecchio, A. Ninfa and E. Sontag, "Modular Cell Biology: Retroactivity and Insulation", *Molecular Systems Biology*, vol. 4, no. 1, 2008.

[14] M. Pedersen and B. Yordanov, "Programming Languages for Circuit Design, Computational Methods in Synthetic Biology", *Methods in Molecular Biology*, vol. 1244, pp. 81–104, Springer, 2014.

[15] M. R. Roussel, "The Use of Delay Differential Equations in Chemical Kinetics", *The Journal of Physical Chemistry*, vol. 100, pp. 8323-8330, 1996.

[16] Y. Shtessel, C. Edwards, L. Fridman, A. Levant, "Introduction: Intuitive Theory of Sliding Mode Control", in *Sliding Mode Control and Observation*, pp. 1–42. Springer New York, 2014.

[17] V. Utkin, "Scope of the Theory of Sliding Modes" in *Sliding Modes in Control and Optimization*, pp. 1–11. Springer Berlin Heidelberg, 1992.

[18] H. Khalil, "Nonlinear Design Tools" in *Nonlinear Systems*, pp. 551–625. New Jersey Prentice Hall, 2002.

[19] M. Feinberg, *Lectures on Chemical Reaction Networks, Notes of Lectures Given at the Mathematics Research Center of the University of Wisconsin*, [Online]. Available: http://www.che.eng.ohio-state.edu/ FEINBERG/LecturesOnReactionNetworks, 1979.

[20] M. Vidyasagar, "Statistical Learning Theory and Randomized Algorithms for Control", *IEEE Control Systems Technology*, vol. 18, no. 6, pp. 69–85, 1998.

[21] P. S. Williams, "*A Monte Carlo Dispersion Analysis of the X-33 Simulation Software*", Proceedings AIAA Conference on Guidance, Navigation and Control, Montreal, Canada, 2001.

[22] P. P. Menon, I. Postlethwaite, S. Bennani, A. Marcos, and D. G. Bates, "Robustness Analysis of a Reusable Launch Vehicle Flight Control Law", *Control Engineering Practice*, vol. 17, no. 7, pp. 751–765, 2009.